Journal of Applied Polymer Science

Joint effects of rotational extrusion and TiO_2 on performance and antimicrobial properties of extruded polypropylene copolymer pipes

Xiao Li, Lin Pi, Min Nie, Qi Wang
State Key Laboratory of Polymer Materials Engineering, Polymer Research Institute of Sichuan University, Chengdu 610065, China
Correspondence to: M. Nie (E-mail: poly.nie@gmail.com)

ABSTRACT: In this study, effects of titanium dioxide (TiO_2) and rotation extrusion on structures and properties of polypropylene random copolymer (PPR) pipes were investigated. The experimental results showed that with the presence of TiO_2, not only the antibacterial ability of PPR pipe was improved significantly but also the toughness was enhanced since a large number of PP chains were promoted to crystallize into β-form crystals. Furthermore, when rotation extrusion was introduced into the process of PPR pipe, the drag hoop flow caused by mandrel and die rotation was superposed on the axial flow, so the polymer melts in the annulus underwent a helical flow and its flow direction deviated from the axis to drive the molecular orientation off the axial direction, bringing out the increased hoop strength. As a result, PPR pipe with excellent performance was prepared under the combined effect of rotation extrusion and TiO_2. The antibacterial activity was 99.2%, the hoop tensile strength reached 27.5 MPa, 67.7% higher than that of the convention-extruded PPR pipe with TiO_2, and the impact strength was 10.9 kJ/m^2, increased by 81.6% compared to that of the rotation-extruded pure PPR pipe. © 2015 Wiley Periodicals, Inc. J. Appl. Polym. Sci. **2015**, *132*, 42410.

KEYWORDS: manufacturing; mechanical properties; properties and characterization

Received 13 December 2014; accepted 23 April 2015
DOI: 10.1002/app.42410

INTRODUCTION

Polypropylene (PP) pipes are widely used as hot and cold water transport pipes due to their comprehensive advantages, such as corrosion resistance, light weight, excellent resistance to thermal distortion, and good mechanical properties.[1–3] Therefore, it is in pressing need to prepare PP pipes with high performance. Performances of polymer products not only are related to the molecular structure but also depend on the multistructures generated during the practice processing.[4] It has been proved to be a feasible and effective way to achieve the improved performances by tailoring orientation and crystalline structure via novel processing technology.[5–7] Generally, polymer melts are drawn along axial direction in convention-extruded PP pipes so molecular orientation is paralleled to the axis and the hoop strength is inferior to the axial one. Unfortunately, when PP pipes are used as water transport pipe, the hoop stress which the pipe is subjected to is at least twice as much as the axial stress.[8] Obviously, the axial molecular orientation in PP pipes is unfavorable to their application. So far, many processing technologies have been proposed to erase axial molecular orientation and improve hoop strength such as solid extrusion,[9] vibration extrusion,[10] and rotation extrusion.[11]

During rotation extrusion, with the superposition of axial flow and drag hoop flow caused by mandrel or die rotation, polymer melts move forward helically. The flow deviated from the axis could drive the molecular orientation off the axial direction to enhance the hoop performance. For example, Nie[12] achieved the shish-kebab morphology off the axial direction in polyethylene (PE) pipe through mandrel and die rotation and prepared PE pipe with high hoop strength. However, the previous work mainly focused on homogenous systems and no information on formation and evolution of hierarchical structure of multiphase systems during rotation extrusion processing is available.

On PP pipe's applications, the commonly used material is polypropylene random copolymer (PPR) since the impact resistance of ordinary isotactic polypropylene is poor. PPR is a copolymer with ethylene molecules randomly inserted along PP chains, where the crystallizable homopolymer sequences endow superior strength while propylene–ethylene random segments gather together to form a rubbery phase and bring out excellent toughness.[13,14] Obviously, as a typical multiphase polymer, the sensitivities of its crystallization behaviors to the stress and temperature are different from homogenous systems, such as PE, isotactic PP. It is worthy of further studying on the rotation extrusion of PPR pipe. Moreover, PPR pipes are poor in the antimicrobial properties, and are liable to mildew under certain temperature and humidity condition. It is not suitable for drinking water

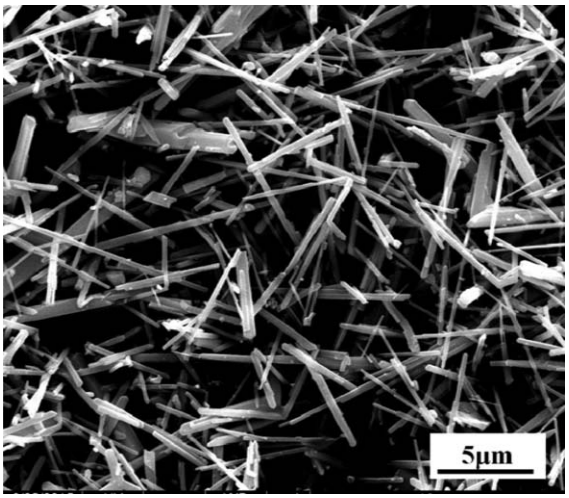

Figure 1. SEM image of TiO_2 powders.

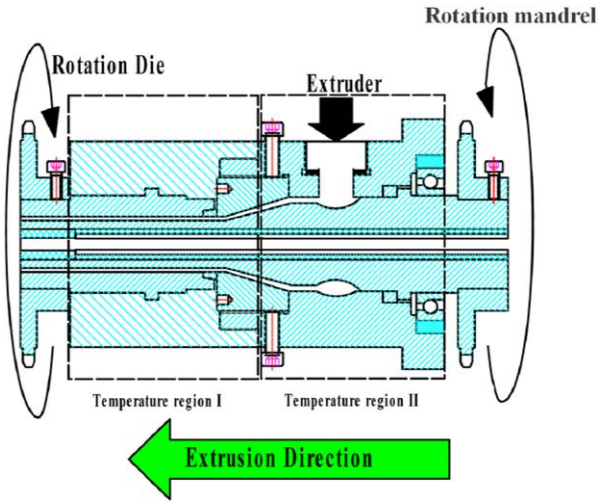

Figure 2. Schematic diagram of polymer pipe's rotation extrusion equipment. [Color figure can be viewed in the online issue, which is available at wileyonlinelibrary.com.]

transport. Introduction of antimicrobial agent is regarded as the most effective and accessible method to improve the antimicrobial property of polymer materials.[15] Among all antimicrobial agents, TiO_2 possesses safety, high activity, strong oxidization, and long-term stability.[16,17] It is evident that TiO_2 not only can be photoactivated by UV light but also has high antibacterial efficacy under visible light.[18] Shieh[19] reported an antibacterial performance of TiO_2 against *Escherichia coli* could reach 99.9% bacterial reduction under activation by visible light. Now, TiO_2 has been successfully applied to visible light-induced inactivation of microorganisms. Compared to UV irradiation, visible light-activated process exhibits wider potential applications and is favorable for the used condition of PPR pipe. Expectedly, under the coupled effects of rotation extrusion and antimicrobial TiO_2, PPR pipes with excellent mechanical performances and antimicrobial properties simultaneously can be prepared.

In this article, certain amount of antimicrobial TiO_2 was introduced into PPR matrix and then was processed into the pipe through the self-designed rotation extrusion system. And a system investigation of multilevel and multiscale structures of PPR pipe through a variety of characterization methods was conducted and the relationship among the processing conditions, structures, and performances was discussed for preparation of PPR pipe with excellent performances.

EXPERIMENTAL

Materials

The polypropylene used in this study was polypropylene random copolymer (Trade Name, R200P), provided by Hyosung Corporation (Korea). Its weight average molecular weight was 72.2×10^4 g/mol and the content of ethylene was 3.8%.

TiO_2 powders (FT-3000) produced by Ishihara Sangyo Corporation (Japan) were used as an antimicrobial agent. As shown in Figure 1, the length and diameter were 4.7 and 0.25 μm, respectively. The specific gravity was 4.3.

Sample Preparation

A mixture of PPR resin and fibrous TiO_2 (weight ratio: 96 : 4) was premixed and subsequently extruded in a twin-screw extruder. The obtained pellets were extruded into PPR pipes via a self-designed rotation extrusion equipment, which had rotatable mandrel and die. Accordingly, during rotation extrusion of PPR pipe, hoop flow induced by mandrel and die rotation was superposed on axial traction flow to change polymer melt from axial flow to helical flow off the axial direction. Its schematic diagram was presented in Figure 2 and the detailed structure was described elsewhere.[6,20] In this study, with the presence of TiO_2, mandrel and die rotated synchronously in the same direction at the speed of 4 r/min during the extrusion of PPR pipe. The prepared PPR pipe was named RTPPR and the outer diameter and wall thickness were 32 and 2 mm, respectively. For comparison, rotation-extruded PPR pipes without TiO_2, convention-extruded PPR pipes with and without TiO_2 were also prepared and named RPPR, CTPPR, and CPPR, respectively.

Characterization

Differential Scanning Calorimetry (DSC) Analysis. The thermal analysis of the samples was conducted to investigate the crystalline structures of the prepared PPR pipes by a Q20 DSC apparatus (TA Instruments), calibrated using indium and zinc standards. Specimens of 5–8 mg were heated from 40 to 180°C under the protection of nitrogen atmosphere and the heating rate was 10°/min.

Wide-Angle X-ray Diffraction (WAXD) Measurement. The crystalline polymorphs of the PPR pipes were investigated by a DX-1000 diffractometer (Dandong Fangyuan Instrument Co., Ltd, China). The CuK_α generator system was operated at 40 kV and 25 mA. The scanning 2θ ranged from 10° to 40° with a scanning rate of 1°/s. The relative amount of β-form crystal in the prepared PPR pipes was calculated according to Tuner–Jones equation:[21]

$$K_\beta = \frac{I_{\beta(300)}}{I_{\beta(300)} + I_{\alpha(110)} + I_{\alpha(040)} + I_{\alpha(130)}} \quad (1)$$

where $I_{\beta(300)}$ was the peak intensity of $\beta(300)$ plane, and $I_{\alpha(110)}$, $I_{\alpha(040)}$, and $I_{\alpha(130)}$ were the peak intensities of $\alpha(110)$, $\alpha(040)$, and $\alpha(130)$ planes, respectively.

Scanning Electron Microscopy (SEM) Observation. The crystal morphology of the PPR pipes was observed by an Inspect F (FEI) SEM instrument at 0.5 Torr and 20 kV. The SEM samples were cut along the axial direction of PPR pipes and put into the permanganic etchant at 50°C for 48 h to remove the amorphous phase. The permanganic etchant used was 1 wt % potassium permanganate solution. Then the etched samples were carefully washed by diluents sulfuric, hydrogen peroxide, and distilled water in sequence and finally gold-sputtered for observation.

Thermal Shrinkage. Thermal shrinkage was conducted to estimate the molecular orientation in the PPR pipes. Along the axial direction, the strips of 2 cm length were cut from PPR pipes, then put into glycerol, and kept at 145°C until no dimensional changes occurred. The strip lengths before and after heating were measured and the shrinkage ratio was calculated according to the ratio of original-to-final dimension after the heating.

Tensile Strength Testing. According to GB/T 1040-92 standard, the hoop strength of the PPR pipes was measured in a universal testing machine (model RG L-10, Shenzhen Reger Instrument Co., Ltd.). The 10-mm-wide rings were cut from the hoop direction of the extruded pipe, and then tested under 20 mm/min constant crosshead movement. The average value of five specimens was reported.

Impact Strength Testing. According to the GB/T1834-1996 standard, the notched Izod impact strength of the PPR pipe was measured on izod machine XBJ-7.5/11 (Chang Chun Testing Machine Co., Ltd.) using bars cut directly along the axial direction of the pipes. The specimens were V-notched with 2 mm depth and kept at 0°C for 12 h before testing.

Antimicrobial Testing. According to the proposed antimicrobial testing method,[22,23] the antimicrobial ability of the PPR pipes was evaluated quantitatively in the fluid nutrient medium composed of beef extract, peptone, sodium chloride, and water with the weight ratio 1 : 2 : 1 : 200.[24,25] First, the fluid nutrient medium was sterilized in an autoclave and then incubated with *Staphylococcus aureus*, a model microorganism commonly used for antibacterial experiments, at 37°C for 5 days. Then, the bacterial colony of *S. aureus* was transferred into nutrient solution and diluted to prepare the testing reagent with concentration 5.0×10^5 cfu/mL (cfu: colony-forming unit). The strips of PPR pipes were coated evenly with the testing reagent and were incubated at 37°C for 24 h in a sterile environment. At last, the *S. aureus* on the surface of the PPR pipes was collected and counted and the antibacterial activity (R) was obtained with the following equation:[26]

$$R(\%) = (A - B)/A \times 100\% \quad (2)$$

where A and B are the *S. aureus* quantities on the surface of blank sample and PPR pipes, respectively.

RESULTS AND DISCUSSION

Effect of Rotation Extrusion and Titanium Dioxide on Performances of PPR Pipe

Tensile strength and impact strength of the four PPR pipes were presented in Figure 3. Clearly, the PPR pipes prepared via rotation extrusion had higher hoop tensile strength than that of convention-extruded ones and introduction of TiO_2 improved the impact strength significantly. However, either rotation extrusion or TiO_2 independently is ineffective enough to simultaneously improve the hoop strength and impact strength of the PPR pipes. For example, the hoop tensile strength of RPPR was 26.8 MPa, higher than 15.3 MPa of CPPR but the impact strength remained unchanged, 6.0–6.4 kJ/m^2. On the contrary, the impact strength of CTPPR reached 10.3 kJ/m^2 but the hoop strength was only 16.4 MPa. Under the combined effects of rotation extrusion and TiO_2, RTPPR had best mechanical performances. Compared to the convention-extruded pure PPR pipe, the hoop tensile strength and impact strength were 27.5 MPa and 10.9 kJ/m^2, increased by 79.7% and 70.3%, respectively.

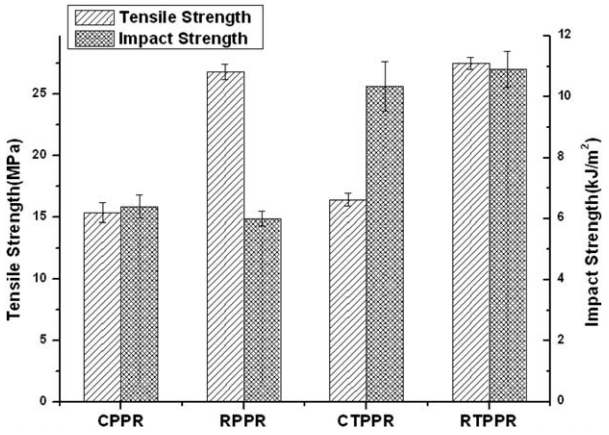

Figure 3. Mechanical properties of PPR pipes without and with TiO_2 prepared via convention extrusion and rotation extrusion.

In addition, the antimicrobial properties of PPR pipes were quantitatively evaluated based on the bacterial quantity grown on the surface of the blank sample and testing sample, which were coated with the testing reagent and incubated at 37°C for 24 h. In this testing method, the antibacterial activity (R) value was a sole parameter to judge the antibacterial property of the testing sample, i.e., the sample of R value higher than 90% was considered as an antibacterial material. The results showed that pure PPR pipes had no antibacterial ability and its antibacterial activity to *S. aureus* was 0. With the presence of TiO_2, *S. aureus* grew on the surface of the PPR pipe was inhibited and the antibacterial activity was 99.2%, indicting the existence of TiO_2 improved the antibacterial ability of PPR pipes.

Effect of Rotation Extrusion and Titanium Dioxide on Structures of PPR Pipe

The crystal and orientation structures of PPR pipes were influenced inevitably by extrusion modes and additives. In this study, a variety of characterization methods were adopted to analyze the combined effect of TiO_2 and rotation extrusion. Figure 4 showed the DSC melting curves for the four PPR pipes prepared under the different conditions. For pure PPR pipes, a single sharp melting peak was displayed at ~140°, indicating only α-form crystals were generated. As for the PPR pipes with TiO_2, the distinct different melting behaviors were observed that there were two melting peaks at 127 and 143°C. The peak

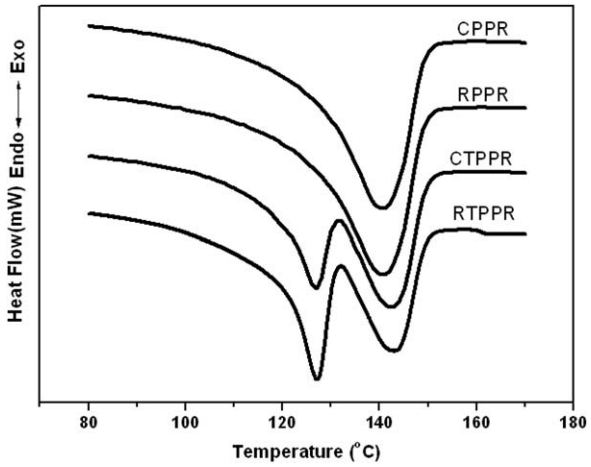

Figure 4. DSC curves of PPR pipes without and with TiO_2 prepared via convention extrusion and rotation extrusion.

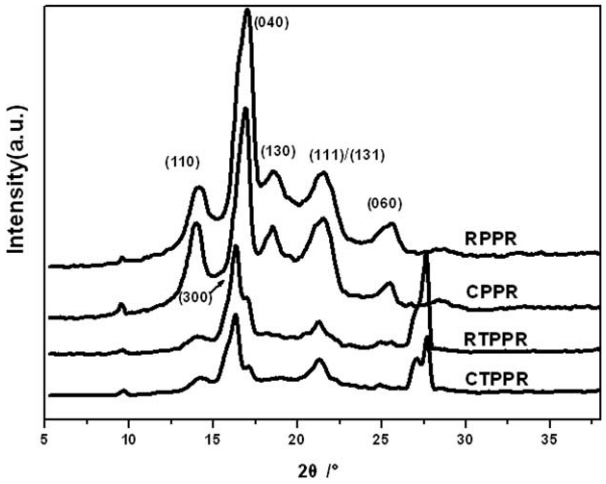

Figure 5. XRD curves of PPR pipes without and with TiO_2 prepared via convention extrusion and rotation extrusion.

located at lower temperature corresponded to β-form crystal while the other at higher temperature should be ascribed to α-form crystal, implying that α and β-form crystals were co-existed with the presence of TiO_2. β-form crystal was a metastable phase and only α-form crystal was produced under normal processing conditions.[27,28] Therefore, the formation of β-form crystal in the PPR pipes suggested that TiO_2 was an effective β nucleating agent for PP. Moreover, the crystallinity for the four PPR pipes were also calculated according to the ratio of the measured enthalpy of fusion and the enthalpy for 100% crystalline (165 J/g). The results showed there were slight influences of rotation extrusion and TiO_2, as shown in Table I.

XRD experiments were further adopted to quantitatively estimate crystalline structures of the PPR pipes. As shown in Figure 5, pure PPR pipes exhibited the four typical diffraction peaks at $2\theta = 14.1$, 16.9, 18.8, and 21.6°, corresponding to the (110), (040), and (130), overlapping (111) and (131) reflection of the α-form crystal, respectively. When TiO_2 was introduced into PPR matrix, additional diffraction peak at $2\theta = 16.1°$, corresponded to the characteristic reflection of the (300) plane of β-form crystal, was identified and its intensity was far higher than any characteristic peaks of α-form crystal, indicating high relative content of β-form crystal was obtained. This was in accord with the DSC results. Based on Tuner–Jones equation, the relative content of β-form crystals in the PPR pipes with TiO_2 was calculated and the results were present in Table I. Apparently, the addition of TiO_2 indeed induced a larger fraction of PP chains to crystallize into β-form crystals. This can be ascribed to good lattice matching between PP and TiO_2. According to the proposition of Huang and coworkers, the additives that exhibited the strongest reflection at the d-spacing of 0.28–0.31 could promote the formation of β-form crystals in PP matrix.[23] Figure 6 showed the XRD curve of TiO_2 powders. The strongest reflection representing (110) plane was located at 27.6° and the d-spacing was calculated to be 0.32 nm. Therefore, it seemed reasonable that numerous β-form crystals were generated in the PPR pipes with the presence of TiO_2. Moreover, for CTPPR and RTPPR, the relative content of β-form crystals reached 57.7 and 63.3%, respectively. Compared to the convention-extruded ones, rotation-extruded PPR pipes had slightly higher β-form crystals. Accordingly, it came into conclusion that under the superposed effect of rotation extrusion and TiO_2, the formation of β-form crystals was promoted greatly.

Crystal morphologies of the PPR pipes were available via SEM examinations. Figure 7 showed the SEM images of the four PPR pipes prepared under different conditions. Clearly, some holes

Table I. DSC and XRD Results of PPR Pipes without and with TiO_2 Prepared via Convention Extrusion and Rotation Extrusion

Samples	ΔH_m (J/g)	$T_{m\alpha}$ (°C)	$T_{m\beta}$ (°C)	X_c (%)	K_β (%)
CPPR	54.0	140.9	-	32.7	0
RPPR	55.5	141.1	-	33.6	0
CTPPR	61.0	143.4	126.9	36.9	56.7
RTPPR	63.0	143.8	127.1	38.1	63.3

ΔH_m: the measured fusion heat; $T_{m\alpha}$: melting peak temperature of α-form crystal; $T_{m\beta}$: melting peak temperature of β-form crystal; X_c: crystallinity obtained based on DSC curves; K_β: relative amount of β-form crystal resulted from XRD results.

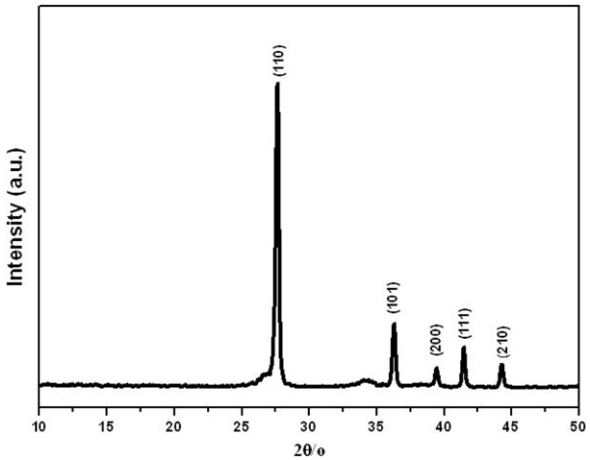

Figure 6. XRD curve of TiO2 powders.

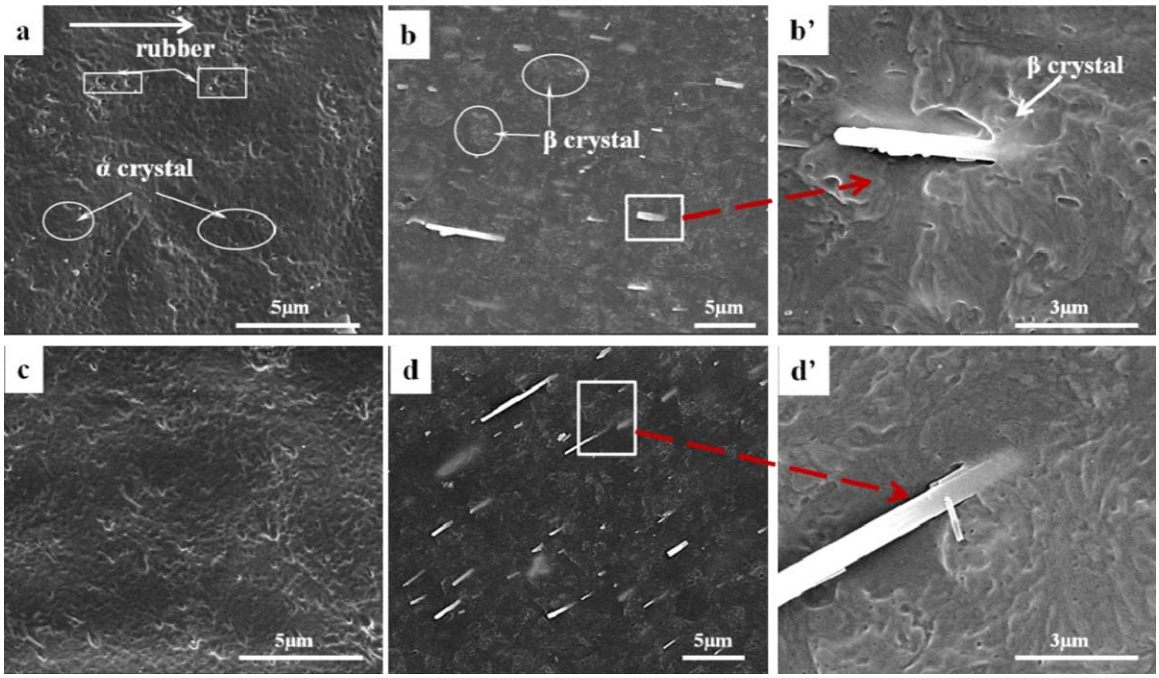

Figure 7. SEM images of PPR pipes prepared by convention extrusion and rotation extrusion. (a) CPPR; (b) CTPPR; (c) RPPR; (d) RTPPR; (b') and (d'): (b) and (d) with higher magnification. The direction of white arrow showed the axial direction. [Color figure can be viewed in the online issue, which is available at wileyonlinelibrary.com.]

were presented on the PPR pipes' etched surface. It is well known that PPR chains contain not only crystallizable polypropylene phase but also some amorphous ethylene–propylene rubber phase. Obviously, there existed a two-phase structure in the PPR pipes, among which the holes represented the amorphous rubber phase removed easily by the etchant. The similar result was also investigated by other researcher.[29] And due to different lamellar stacking patterns between α-form crystal and *β*-form crystal, after selective etching, the exposed structure of dense α-form crystal is feint while the loose structure of *β*-form crystal can be etched deeply.[30] The two kinds of crystals can be distinguished through SEM observation.[31] Distinctly, the four PPR pipes exhibited spherulites structure and no oriented crystals. However, only α-form crystal was shown in pure PPR pipes. In contrast, PPR pipes with TiO_2 contained two form crystals and *β*-form crystal mainly grew epitaxially on the surface of TiO_2 [Figure 7(b',d')], indicating TiO_2 indeed had the pronounced influence on the formation of *β*-form crystals. Moreover, it was obvious that TiO_2 was distributed uniformly in the PPR pipes [Figure 7(b,d)] and extrusion modes affected the alignment of fibrous TiO_2 in the PPR pipes. Convention extrusion induced the TiO_2 oriented along the axial direction while the alignment of TiO_2 in the PPR pipe prepared via rotation extrusion was off the axial direction.

Thermal shrinkage experiments were also carried out to investigate the molecular orientation in various PPR pipes. When an oriented sample is heated above its melting temperature, the oriented molecules will go back to the random coiled state and thus the length along the orientation direction will shorten. Therefore, the shrinkage ratio can be considered as an indicator of molecular orientation.[32] For the sample with higher orientation, the shrinkage ratio is higher. Figure 8 showed the photographs of the strips with original 20 mm length after heated. The axial sizes of CPPR, CTPPR, RPPR, and RTPPR were 10, 12, 15, and 18 mm, respectively. Clearly, the axial shrinkages of convention-extruded PPR pipes were more than that of rotation extruded PPR pipes, implying rotation extrusion could suppress the axial orientation of molecules. This is a key for PPR pipe with high hoop strength.

Relation Among Extrusion Modes, Structure, and Performances

The properties of polymer materials not only depend on their chemical structure but also are related to the morphology and nature of the crystalline phase developed during the processing.[4,33] For example, molecular orientation can improve the strength of polymer products along the oriented direction while *β*-form crystals can bring out high toughness.

For common isotactic polypropylene, its impact resistance is low. To solve this issue, ethylene molecules is introduced into the PP chains through new copolymerization technology to endow excellent toughness. However, the enhanced toughness is at the expense of its high strength. On the other hand, during the convention extrusion, the molecular chains flow along the axial direction so the molecular orientation is paralleled to the axis and the prepared pipes have poor hoop strength. As shown in Figure 3, the hoop strength of the convention-extruded pure PPR pipe was only 15.3 MPa. But in PPR pipes' application, higher hoop strength is required since hoop stress is twice higher as axial stress. Therefore, it is important to prepare PPR pipes with excellent hoop strength by tailoring molecular orientation off the axial direction.

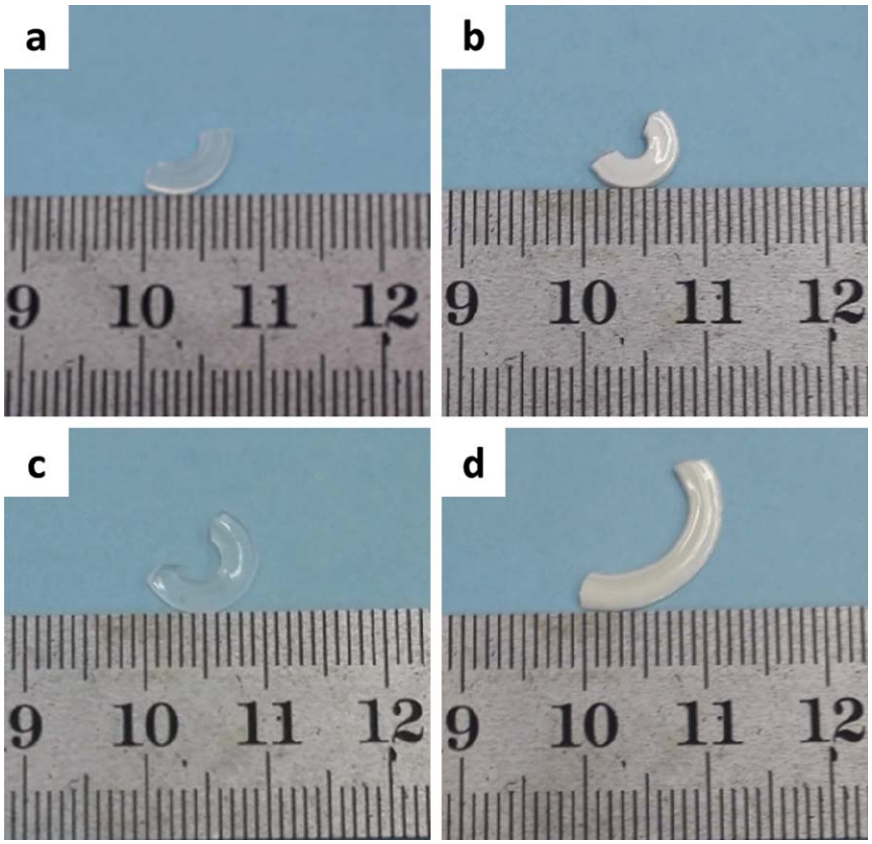

Figure 8. Photographs of the strips from PPR pipes along the extrusion direction after 1 h annealing at 145°C. (a) CPPR; (b) RPPR; (c) CTPPR; (d) RTPPR. [Color figure can be viewed in the online issue, which is available at wileyonlinelibrary.com.]

In this study, self-designed rotation equipment was adopted. With the mandrel and die rotation, a hoop flow was superposed on the axial flow and the flow pattern of the polymer melts in die changed from the axial flow to helical flow in an off-axis direction. Generally, flow direction of polymer melts determines that of molecular orientation. Accordingly, the molecular orientation deviated from the axial direction during rotation extrusion. From the thermal shrinkage results, the PPR pipes prepared via rotation extrusion had lower axial orientation so the hoop strength was higher. Different from the former work on PE pipe, no oriented shish-kebab crystals were generated and the four PPR pipes exhibited isotropic spherulites. It can be ascribed to the weak crystallization ability of PPR caused by the confined effects of the ethylene–propylene rubber phase on the movement of PP chains, which was proved by only ~33% crystallinity of all PPR pipes. Thus, no oriented-crystal morphology was generated in the PPR pipes. Other researchers also investigated and proved that it is difficult for PPR to generate shish-kebab even at the intense stress.[34,35]

Although TiO_2 dispersed uniformly in PPR pipes, nevertheless, the expected reinforcing effects of the rigid fibrous TiO_2 on the PPR pipes were not observed. This is because the reinforcing effects depend on the alignment of additives, which was determined by the direction of the flow. During the convention extrusion, the fibrous TiO_2 preferred to align along the axial direction while the alignment of TiO_2 deviated off the axial direction in the rotation extrusion of PPR pipes, as shown in Figure 7. Obviously, the latter had better hoop reinforcing effects on the PPR pipes. However, based on the DSC and XRD results, TiO_2 was an efficient β-nucleating agent for PP due to their matching lattices. With the presence of TiO_2, the content of β-form crystals increased significantly. Compared to α-form crystals, β-form crystals were favorable to enhance the impact toughness of PP but reduce the strength. As a result, rotation-extruded PPR pipe with TiO_2 exhibited higher impact strength and almost the same hoop strength as pure PPR pipe prepared in the same conditions. As shown in Figure 3, RTPPR had best mechanical performances under the synergistic effects of rotation extrusion and TiO_2.

More importantly, TiO_2 is one of the most powerful photocatalytic materials and can be activated by visible light to generate some reactive oxygen species with strong oxidizing power (•OH and $O_2^{\bullet -}$, etc.).[36] Subsequently, the oxidizing species can kill organic species with mineralization producing CO_2 and H_2O.[18] Therefore, introduction of TiO_2 also increased the antimicrobial properties of PPR pipes.

CONCLUSION

In this study, PPR pipe containing fibrous TiO_2 was prepared via a self-designed rotation-extrusion equipment and its structure and performances were investigated. The results showed that rotation extrusion did not change the crystal morphology

in the prepared PPR pipes but induced the molecular chains deviated from the axial direction. Compared to the axial orientation in convention-extruded one, the orientation off the axis could improve the hoop tensile strength. Moreover, TiO_2 not only acted as an efficient β-nucleating agent to promote the formation of β-form crystals and enhance the impact strength, but also had antimicrobial ability to inhibit bacteria's activity and increase the antibacterial activity of PPR pipes. Obviously, neither rotation extrusion nor TiO_2 independently was effective enough to improve the hoop strength and impact strength of the PPR pipes simultaneously. For example, the hoop tensile strength of RPPR was 26.8 MPa, higher than 15.3 MPa of CPPR but the impact strength remained unchanged, 6.0–6.4 kJ/m^2. On the contrary, the impact strength of CTPPR reached 10.3 kJ/m^2 but the hoop strength was only 16.4 MPa. Under the combined effects of rotation extrusion and TiO_2,[13] RTPPR had best mechanical performances. The antimicrobial property was enhanced and the hoop tensile strength and impact strength reached 27.5 MPa and 10.9 kJ/m^2, increased by 79.7 and 70.3%, respectively, compared to the convention-extruded pure PPR pipe.

ACKNOWLEDGMENTS

This work is financed by the National Natural Science Foundation of China (51127003, 51303114, and 51421061) and the Doctoral fund of Ministry of Education of China (20130181120056).

REFERENCES

1. Remias, J. *Intern. Polyolefins Confern.* **2009**, *519*, 2009.
2. Yayla, P.; Sahin, S. *Polym. Test.* **2005**, *24*, 1012.
3. Chen, K. Y.; Zhou, N. Q.; Liu, B.; Jin, G. *J. Appl. Polym. Sci.* **2009**, *114*, 3612.
4. Rajesha, S.; Venkatesh, G.; Sharma, A. K.; Kumar, P. *Indian. J. Eng. Mater. S.* **2010**, *17*, 407.
5. Bunget, C.; Ngaile, G. *Ultrasonics.* **2011**, *51*, 606.
6. Liu, W.; Wang, Q.; Nie, M. *J. Polym. Eng.* **2014**, *34*, 15.
7. Mousavi, S.; Feizi, H.; Madoliat, R. *J. Mater. Process. Technol.* **2007**, *187*, 657.
8. Williams, J. G.; Hodgkinson, J. M.; Gray, A. *Polym. Eng. Sci.* **1981**, *21*, 822.
9. Sawai, D.; Takahashi, K.; Imamura, T.; Nakamura, K.; Kanamoto, T.; Hyon, S. H. *J. Polym. Sci. Part B: Phys.* **2002**, *40*, 95.
10. Gao, X. Q.; Zhang, J.; Chen, C. S.; Shen, K. Z. *J. Appl. Polym. Sci.* **2007**, *106*, 552.
11. Han, R.; Nie, M.; Bai, S. B.; Wang, Q. *Polym. Bull.* **2013**, *70*, 2083.
12. Nie, M.; Wang, Q. *J. Appl. Polym. Sci.* **2013**, *128*, 3149.
13. Geng, C. Z.; Yang, G. H.; Bai, H. W.; Li, Y. H.; Fu, Q.; Deng, H. *J. Supercrit. Fluids.* **2014**, *87*, 83.
14. Duvall, D. *J. Fail. Anal. Preven.* **2014**, *14*, 336.
15. Kangwansupamonkon, W.; Lauruengtana, V.; Surassmo, S.; Ruktanonchai, U. *Nanomed-nanotechnol.* **2009**, *5*, 240.
16. Mitoraj, D.; Janczyk, A.; Strus, M.; Kisch, H.; Stochel, G.; Heczko, P. B.; Macyk, W. *Photochem. Photobiol. Sci.* **2007**, *6*, 642.
17. Barletta, M.; Vesco, S.; Tagliaferri, V. *Colloids Surfaces B: Biointerfaces* **2014**, *120*, 71.
18. Pelaez, M.; Nolan, N. T.; Pillai, S. C.; Seery, M. K.; Falaras, P.; Kontos, A. G.; Dunlop, P. S. M.; Hamilton, J. W. J.; Byrne, J. A.; O'Shea, K.; Entezari, M. H.; Dionysiou, D. D. *Appl Catal B-Environ.* **2012**, *125*, 331.
19. Yau-Chyr, W.; Kuan-Jiunn, S.; Min, L.; Yu-Hwe, L.; Shinn-Der, S.; Yu-Tsung, L. *Nanomed. Nanotechnol. Biol. Med.* **2006**, *2*, 121.
20. Wang, Q.; Zhang, J.; Guo, Y.; Bai, S. B.; Hua, Z. K. ZL200810045785.9, **2010**.
21. Li, Y. J.; Wen, X. Y.; Nie, M.; Wang, Q. *J. Appl. Polym. Sci.* **2014**, *131*, 9.
22. Li, M.; Li, G.; Jiang, J.; Tao, Y.; Mai, K. *Compos. Sci. Technol.* **2013**. *81*, 30.
23. Li, M.; Li, G.; Fan, Y.; Jiang, J.; Ding, Q.; Dai, X.; Mai, K. *Polym. Bull.* **2014**, *71*, 2981.
24. Pline, W. A.; Lacy, G. H.; Stromberg, V.; Hatzios, K. K. *Pestic. Biochem. Physiol.* **2001**,*71*,48.
25. De Oliva Neto, P.; Ferreira, M. A.; Yokoya, F. *Bioresour. Technol.* **2004**, *92*, 1.
26. Jiang, J.; Li, G.; Ding, Q.; Mai, K. *Polym. Degrad. Stab.* **2012**, *97*, 833.
27. Chang-Mou, W.; Ming, C.; Karger-Kocsis, J. *Polymer* **1999**, *40*, 4195.
28. Somani, R. H.; Hsiao, B. S.; Nogales, A.; Fruitwala, H.; Srinivas, S.; Tsou, A. H. *Macromolecules* **2001**, *34*, 5902.
29. Gahleitner, M.; Tranninger, C.; Doshev, P. *J. Appl. Polym. Sci.* **2013**, *130*, 3028.
30. Feng, L.; Yanling, Z.; Ke, W.; Hua, D.; Feng, C.; Qin, Z.; Qiang, F. *Polymer* **2012**, *53*, 4861.
31. Varga, J. *J. Macromol. Sci. B* **2002**, *41*, 1121.
32. Bornarel, A. C.; White, J. R. *Polym. Polym. Compos.* **1998**, *6*, 287.
33. Wienk, M. M.; Turbiez, M.; Gilot, J.; Janssen, R. A. *J. Adv. Mater.* **2008**, *20*, 2556.
34. Yong, W.; Yao, G.; Jing, S. *J. Appl. Polym. Sci.* **2008**, *107*, 309.
35. Shijie, S.; Peiyi, W.; Jiachun, F.; Mingxin, Y.; Yuliang, Y. *Polymer* **2009**, *50*, 286.
36. Pathakoti, K.; Morrow, S.; Han, C.; Pelaez, M.; He, X.; Dionysiou, D. D.; Hwang, H. M. *Environ. Sci. Technol.* **2013**, *47*, 9988.